





## ORIGINAL RESEARCH ARTICLE

## Characterization and Efficacy Studies of Activated Charcoal Produced from Animal Bones for Heavy Metal Adsorption from Waste Water Using Concentrated Hydrochloric Acid as Activating Agent

Mohammed Shirama Yakubu<sup>1</sup>, Awwal Hussain Nuhu<sup>2</sup>, Yahaya Mohammed Katagum<sup>3</sup>, Abdulrazaq Sanusi<sup>4</sup>

<sup>1</sup>Department of Chemistry, Federal College of Education, Katsina - Nigeria

<sup>2</sup>Department of Chemistry, Bauchi State University, Gadau - Nigeria

<sup>3</sup>Department of Clinical Pharmacy, Faculty of Pharmaceutical Sciences, Bauchi State University, Gadau-Nigeria

<sup>4</sup>Department of Pharmaceutical and Medicinal Chemistry, Faculty of Pharmaceutical Sciences, University of Ilorin, Kwara State - Nigeria

### ABSTRACT

This research work is designed to study and analyse the efficacy and also characterization of the activated charcoal produced from cow, sheep, and goat bones using concentrated hydrochloric acid as an activating agent for toxic metals adsorption using chromatographic techniques. This research aims to provide an eco-friendly adsorbent that will also reduce environmental waste from being converted to activated charcoal. The bones undergo carbonization with the aid of a furnace for one hour (1hr) at 600°C. The bone charcoal was activated with concentrated hydrochloric acid for a period of 4 hrs at a ratio of 10.0 ml per 50.0 g. The activated bone charcoals produced were characterized using scanning electron microscope (SEM) and infrared spectroscopy (FT-IR) before and after adsorption; the results obtained from SEM show the porosity owing to the breakage in the surface of the adsorbents before adsorption while after adsorption the porosity reduces for both adsorbents. The FT-IR results indicated the existence of functional groups OH, C-H, C=O, and PO<sub>4</sub><sup>3-</sup> with some changes in the vibration frequency before and after adsorption. Column adsorption shows that the percentage adsorption for both metals increases with an increase in initial metal concentrations. As the concentration of Lead increased from 20, 30 to 40ppm, there was a corresponding swift increase in adsorption from 46.2 %, 61.58 % to 71.13 % for ACBC (Activated Cow Bone Charcoal) and increase from 25.13 %, 35.65 % to 57.70 % for ASBC. For Copper, there was an increase in adsorption from 37.30 %, 55.90 % to 64.53 % for ACBC, 39.10 %, 56.55 % to 64.90% for ASBC (Activated Sheep Bone Charcoal), for Zinc there was an increase from 35.60%, and 56.45% to 67.03% and similarly for Iron 16.60%, 45.03% to 58.53% for ACBC. The equilibrium data for ASBC-Pb, ACBC-Fe, and ASBC-Fe with a high regression coefficient value (R<sup>2</sup>) of 0.999 each fit well with the Langmuir isotherm model. For ACBC-Pb, ACBC-Cu, ASBC-Cu, ACBC-Zn, and ASBC-Zn with high regression coefficient values (R<sup>2</sup>), 0.999, 1.0, 0.999, 0.999, and 1.0, respectively, fit well to the Freundlich isotherm model. Therefore, the adsorption occurs through multilayer formation on the adsorbent surfaces. The indices of the separation factor K<sub>L</sub> for Langmuir indicate that the adsorption processes are favourable, with the exception of ASBC-Fe, which is unfavourable. The Freundlich isotherm constant n<sub>f</sub> for the adsorption of ACBC-Pb, ACBC-Cu, ASBC-Cu, ACBC-Zn, and ASBC-Zn displays adsorption on heterogeneous surfaces. This uncovers that bone charcoals can be used for the removal of heavy metals by adsorption from aqueous media and can serve as an efficient adsorbent for water purification and treatments in industries.

### ARTICLE HISTORY

Received May 03, 2024

Accepted December 20, 2024

Published December 27, 2024

### KEYWORDS

Activated Charcoal, Animal Bones, Adsorption, Hydrochloric Acid, Heavy Metals



© The authors. This is an Open Access article distributed under the terms of the Creative Commons Attribution 4.0 License

(<http://creativecommons.org/licenses/by/4.0>)

### INTRODUCTION

The studies of wastewater containing toxic metals are considered crucial in the present world. This is due to their impending danger to the environment as a whole. According to World Health Organization (WHO, 2001), toxic metals are harmful even when present in small

concentrations and also instigate different types of illnesses, as reported by *Lourie et al., (2010)*. The various industrial sectors which excessively use water use produce huge flows of industrial waste water. Thus, the waste waters are highly heterogeneous, both quantitatively and

**Correspondence:** Awwal Hussain Nuhu. Department of Chemistry, Bauchi State University, Gadau PMB 065, Bauchi State, Nigeria. ✉ [awwalhussain@basug.edu.ng](mailto:awwalhussain@basug.edu.ng). Phone Number: +234 803 515 3609

**How to cite:** Yakubu, M. S., Nuhu, A. H., Katagum, Y. M., & Sanusi, A. (2024). Characterization and Efficacy Studies of Activated Charcoal Produced from Animal Bones for Heavy Metal Adsorption from Waste Water Using Concentrated Hydrochloric Acid as Activating Agent. *UMYU Scientifica*, 3(4), 408 – 419. <https://doi.org/10.56919/usci.2434.035>

qualitatively, subject to the process applied. These processes often present a wide range spectrum of chemical pollutants (organic or inorganic) with different levels of toxicity that continuously vanish undetected and also not reported. Heavy metals are always considered a threat to the environment, especially when present in water bodies. This is due to their potential harm to the aquatic life and also others who make use of water from such contaminated sources. The effect of consuming water containing heavy metals like Cd has been established to be related to cancerous growth, hormonal disorders, and renal failure (Jorie *et al.*, 2010).

Pollution caused by heavy metals such as Cr, Cu, Pb, Hg, Ni, and Ar poses the highest threat to human health, as reported by Saad *et al.* (2008). Hg is considered to be mutagenic, teratogenic, as well as advanced tyrosinemia. High levels of Hg are linked with serious deficiency of pulmonary and kidney function, chest pain, and dyspnea. Hg poisoning also results in Minamata diseases due to the consumption of fish from Hg-contaminated water bodies (Saad *et al.*, 2008). The efficient treatment of heavy metals is therefore necessary for the safety and optimal performance of the ecosystem. Different research has been documented on how to mop up heavy metals from contaminated water bodies. These methods include coagulation and flocculation, photocatalyst, and membrane filtration processes, as reported by Ahmed *et al.* (2015) and Idris *et al.* (2010), among other researchers.

Currently, adsorption is globally acknowledged as one of the environmental remediation methods. Liquid-solid adsorption systems are based on the capability of certain solids to specifically congregate specific substances from solution onto their surfaces. This principle could be employed to mop up contaminants, like organic and inorganic matter, from wastewater (Kenith & Mekay, 2008). In recent decades, extensive research has been conducted to find inexpensive adsorbents with high efficiency for the removal of metal ions. Several adsorbents have been produced and analyzed, which include quite a lot of activated carbon (Yildiz, 2004).

Activated carbon is among the commonly employed adsorbents to mop metal ions and organic pollutants. The evolution of this technique has been the subject of several experimental studies over a period of time. These adsorbents could be produced from different natural sources, including coal, lignite, anthracite, fibers of palm trees, oil shale, coconut, pea wood, and bone, among others (Alicia *et al.*, 2012).

Water pollution by toxic heavy metals as a result of the release of untreated or poorly treated wastewater from industries, agricultural run-offs, and municipal sectors is a global predicament and also an important source of concern for environmental investigators. The recent fast-recorded industrial development and the amplified population have seriously played a role in the release and subsequent accumulations of As, Cd, Cr, Pb, Cu, Ni, Zn, and Hg, which are toxic to water bodies and, specifically,

to the aquatic lives. These toxic metals can be segregated from other pollutants since they cannot be biodegraded and, consequently, become crowded alongside the food chain. Little industries are guilty of the release of heavy metals into the environment in their effluents (Braukmann, 1990). These industries are considered the main sources of heavy metals and other inorganic contaminants in the environment. Due to the documented evidence on the environmental and health risks of heavy metals, it is considered a duty of these industries to reduce their concentrations to safe limits prior to discharge.

The release of hazardous compounds impacts the quality of water bodies as well as the aquatic lives therein. Thus, researchers have investigated various techniques to proffer solutions. The various methods include chemical oxidation, sedimentation, coagulation and flocculation, membrane filtration, adsorption, and biodegradation. Among the aforementioned methods, adsorption is a well-established method for water cleaning (Moshood *et al.*, 2024). According to Handayani *et al.*, 2024 activated carbon can function as an adsorbent material due to its large specific surface area, capacity adsorption size, structure, type of pore, and reactivity on various surfaces. Zulaikha *et al.*, 2023 have proven that activated carbon (AC) derived from bone char has a porous structure, ease of use, affordability, and ability to function well in a variety of temperatures and humidity conditions. Low-cost adsorbents such as sawdust, banana pith, peanut hull, coir pith, wheat bran, and fruit shells have been employed effectively (Moshood *et al.*, 2024). Animal charcoal, also referred to as bone black, bone char, or abaiser, is a granular material obtained by charring animal bones (Nwankwo *et al.*, 2024).

Activated carbon is known to be used in water treatments of wastewater, and drinking water purification. Similarly, activated carbon is used to remove heavy metals and organic contaminants from liquids. Activated carbon is also used in medicine for adsorption of harmful chemicals and drugs. It is used in de-colourization, deodorization, and taste removal in confectionaries (Isaial and Frank, 2024).

Though activated carbon is usually available, it is still very expensive. Activated carbon could be obtained from organic materials such as plants and animals. In this research, activated carbon will be extracted from cow bones. A way of converting environmental waste to something useful that will be helpful in cleaning the environment.

## MATERIALS AND METHODS

All the reagents used in this research were of analytical grade and were used without further treatment. The apparatus was thoroughly washed with detergents, rinsed with tap water, rinsed again with distilled and deionized water, and dried in an oven at 50° C for 2 hrs. The instruments were also properly calibrated before being used.

### Sample preparation

#### Carbonization of the bones

The bones used for this work were obtained from three different animals, that Cow, a Sheep, and a Goat, and were obtained from an Abattoir in Azare. Firstly, the bones were degreased with boiling water in a cooking pot for 1 hour and dried in a steam room at 110 °C. The bones are then placed in a closed vase and introduced in a furnace at 600 °C in the absence or limited presence of oxygen (Gumus *et al.*, 2012). The carbonized material was recovered after 1 hour of carbonization. The coals obtained were kept in a closed flask to prevent any interaction with air. The carbonized materials were then ground in a mortar and sieved in order to have uniform particles. (Gumus *et al.*, 2012).

#### Activation of the charcoal

The activation of bone charcoal was achieved using concentrated hydrochloric acid as an activating agent with a ratio of 10ml per 50g and a contact time of 4 hours. The carbons were washed with distilled water till a neutral medium (pH=7) was attained. This is done to remove the remains of acid, then filtered with the aid of a vacuum pump and dried at 100 °C in an oven for 2 hours. The powdered activated charcoal acquired was used for the adsorption analysis.

#### Preparation of metal ions standard solution

A stock solution of metal ions (1000 mg/l) was formulated by dissolving the metal salt in deionized water, as described by Gumus *et al.* (2012).

### Adsorption experiment

#### Column adsorption chromatography

A column analysis was carried out with an ordinary 50 mL burette made up of borosilicate glass, which has an internal diameter of 2 cm and a height of 55 cm. The influences of bed height on the breakthrough curve were analyzed by altering the bed height from 5 cm to 10 cm. The bottoms of the columns were corked in with cotton wool to serve as a support and also a stopper for the bone charcoal to avert its floating from the outlet. The column was loaded with the required quantity of bone charcoal to the needed position of the column (5cm and 10cm). The columns were then run in such a manner that an estimated quantity of metal ion solution of requisite concentration

was isocratically added to it using a measuring cylinder and letting it flow along gravity in downflow mode with a steady rate. The rates of flow were examined by evaluating the concentration of metal ions solution in ml flowing per minute periodically. Once the column started, the eluents were received intermittently by means of reagent bottles. These processes were sustained until the column was drained, and the amount of metal ions in different samples was then examined for residual metal ions concentrations. Other similar column techniques were also experimented with for metal ion removal by varying the bed height (5 cm and 10 cm). All the columns were operated at room temperature and a neutral pH of 7.0. The flow rate of the column, removal percentage, and the adsorbent capacity of the adsorbents at different concentrations were calculated.

#### Characterizations of activated charcoals

The following instrument characterized the structural morphology of the adsorbent.

##### Scanning electron microscopy (SEM)

SEM was used to investigate the influence of activation on porosity and also to study the physical surface morphology of the activated charcoal before and after adsorption. The scanning electron micrographs depict the illustrative morphology of the topographical microstructures of the adsorbent (Nwankwo *et al.*, 2018).

##### Fourier transform infrared spectroscopy (FTIR) analysis

The activated charcoal before and after absorption was subjected to an FT-IR spectrometer. The spectra were interpreted. The method used was adapted as described by Nwankwo *et al.* (2018).

### RESULTS AND DISCUSSION

#### Fourier Transform Infrared (FTIR) Spectroscopy

The FTIR analysis of the adsorbents was carried out between 4000 – 100cm<sup>-1</sup> in order to reveal the vibrational frequency changes of the functional groups in the adsorbents. Table 1 shows FTIR spectra of activated cow borne (ACBC) before and after adsorption, while Table 2 shows FTIR spectra of activated sheep bone (ASBC) before and after adsorption. Table 3 shows the FTIR spectra of AGBC before and after adsorption, respectively.

**Table 1: Interpretation of FTIR peaks observed on ACBC before and after adsorptions**

Frequency (cm <sup>-1</sup> )	Before adsorption	After adsorption	Functional groups
3500-3200	3536	-	O-H Stretching (3500 -3200cm <sup>-1</sup> )
1470 -1450	1451	-	C-H bend of alkanes (1470 – 1450 cm <sup>-1</sup> )
1670 -1630	-	1640	C=O Stretching in tertiary amides (1670 -1630 cm <sup>-1</sup> )
1440 – 1400	1413	1410	OH in the carboxylic acid group due to in-plane OH bending (1440 – 1400 cm <sup>-1</sup> )
877	877	877	Presence of aromatic ring



Sample ID:	ACBC Before Adsp	Method Name:	Default
Sample Scans:	32	User:	admin
Background Scans:	32	Date/Time:	5/25/2021 4:29:22PM
Resolution:	8 cm-1	Range:	4,000.00 - 650.00
System Status:	Good	Apodization:	Happ-Genzel
File Location:	C:\Program Files\Agilent\MicroLab PC\Results\ACBC Before Adsp_2021-05-25T16-30-26.a2r		

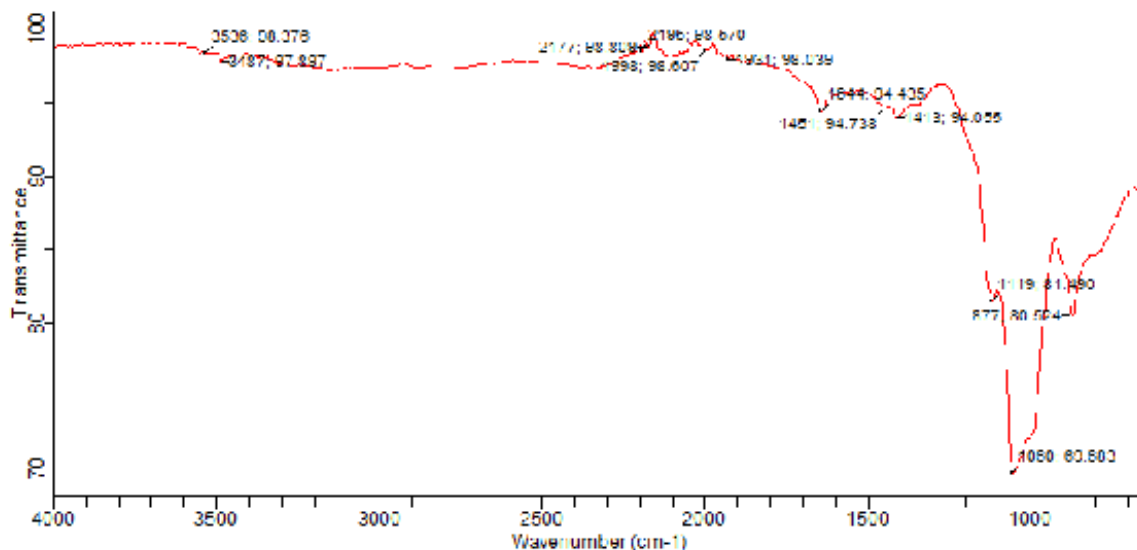


Figure 1: FTIR Spectrum of ACBC before Adsorption



Sample ID:	ACBC After Adsp	Method Name:	Default
Sample Scans:	32	User:	admin
Background Scans:	32	Date/Time:	5/25/2021 4:36:19PM
Resolution:	8 cm-1	Range:	4,000.00 - 650.00
System Status:	Good	Apodization:	Happ-Genzel
File Location:	C:\Program Files\Agilent\MicroLab PC\Results\ACBC After Adsp_2021-05-25T16-36-56.a2r		

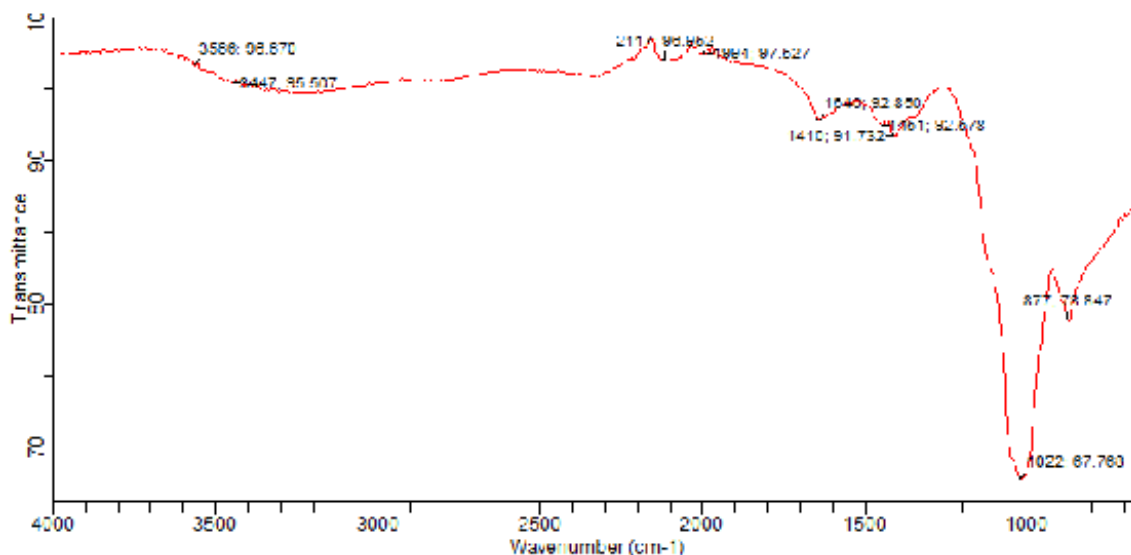
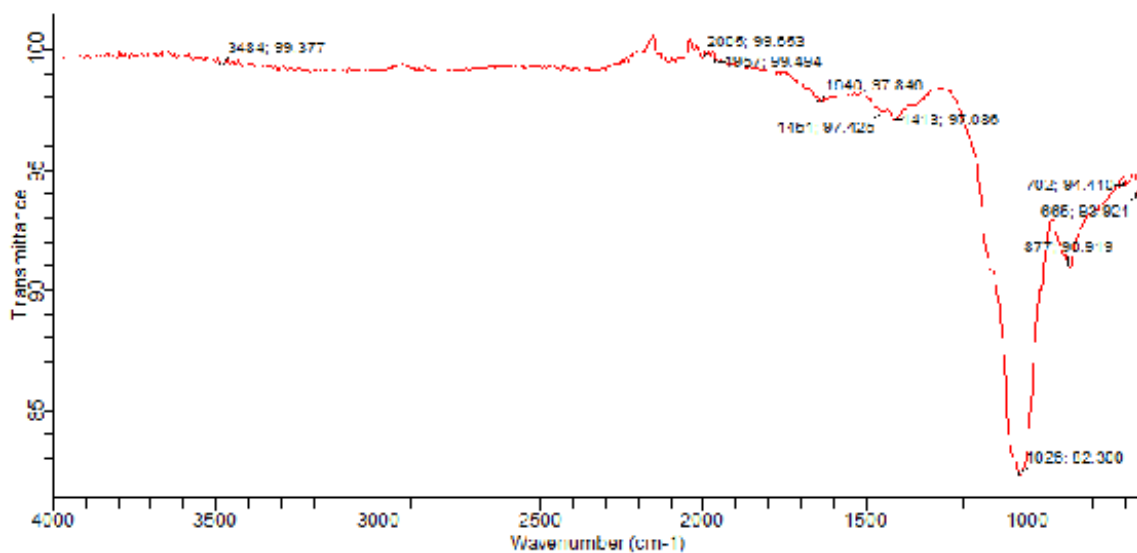


Figure 2: FTIR Spectrum of ACBC after Adsorption



Sample ID:	ASBC Before Adsp	Method Name:	Default
Sample Scans:	32	User:	admin
Background Scans:	32	Date/Time:	5/25/2021 4:34:50PM
Resolution:	8 cm-1	Range:	4,000.00 - 650.00
System Status:	Good	Apodization:	Happ-Genzel
File Location:	C:\Program Files\Agilent\MicroLab PC\Results\ASBC Before Adsp_2021-05-25T16-35-11.a2r		



05/25/2021 16:35:23 Printed by:admin ASBC Before Adsp\_2021-05-25T16-35-11.a2r Page 1 of 1

Figure 3: FTIR Spectrum of ASBC Before Adsorption



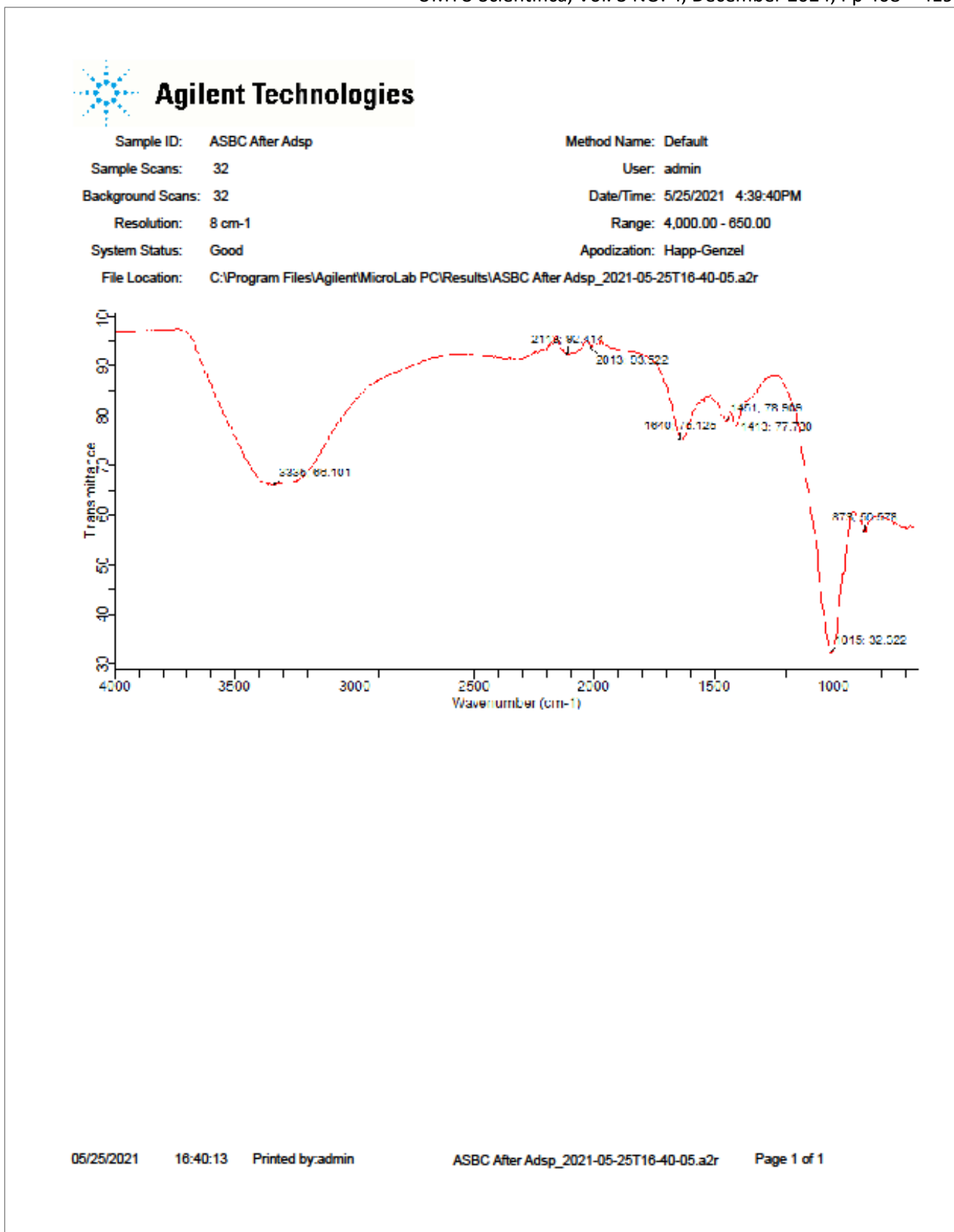


Figure 4: FTIR Spectrum of ASBC After Adsorption

Table 2: Interpretation of FT-IR peaks observed on ASBC before and after adsorptions

Frequency (cm-1)	Before adsorption	After adsorption	Functional groups
3330-3270	-	3331	C-H Stretch

*To be continued next page*

Table 2 Continued

Frequency (cm <sup>-1</sup> )	Before adsorption	After adsorption	Functional groups
1670 -1630	-	1603	C=O Stretching in tertiary amides (1670 -1630 cm <sup>-1</sup> )
1410 -1417	1413	1417	OH in the carboxylic acid group due to in-plane OH bending (1440 – 1400 cm <sup>-1</sup> )
873	873	873	Presence of aromatic ring

**Fourier Transform Infrared (FT- IR) Spectroscopy**

The results obtained from Table 1 show FT-IR spectra of Activated Cow borne (ACBC) before and after adsorption, while Table 2 shows FT-IR spectra of Activated Sheep bone (ASBC) before and after adsorption, respectively. In Table 1, the peaks observed at 1410cm<sup>-1</sup> indicate of existence of a bonded hydroxyl group. The peaks around 1451, 1640, 1410, and 877cm<sup>-1</sup> were assigned to C-H, C=O, OH, and aromatic ring stretching, respectively. In Table 2, the peaks observed at 3335, 1640, 1413, 873, and 541 indicate the presence of OH, C=O, C-H, and aromatic rings, respectively. The additional and oversight peaks and changes in vibrational frequencies after the adsorption of metal ions indicate that adsorption has taken place (Slimani *et al.*, 2013).

**Morphology**

The surface morphology of the adsorbents before and after absorption was observed by SEM for ACBC in Figure 1 and 2 and ASBC in Figure 3 and 4.

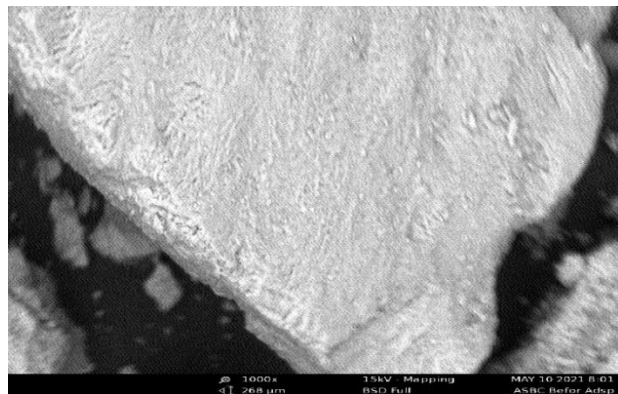


Figure 7: SEM image of ASBC before adsorption

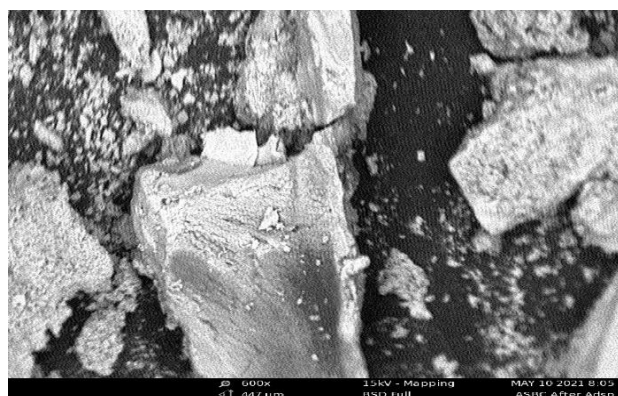


Figure 8: SEM image of ASBC after adsorption

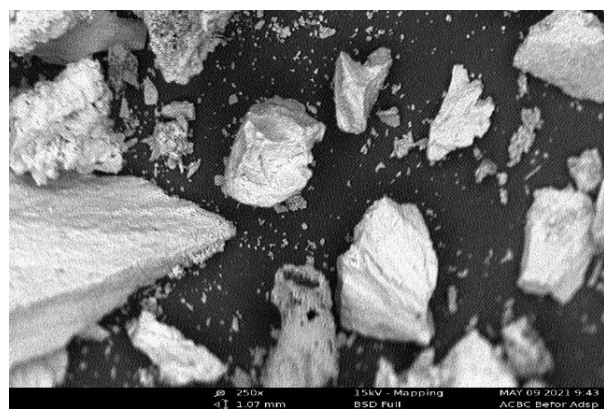


Figure 5: SEM image of ACBC before adsorption



Figure 6: SEM image of ACBC after adsorption

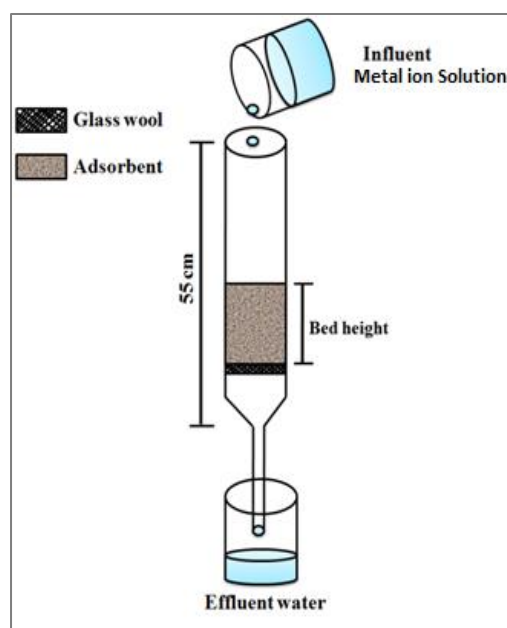


Figure 9: Schematic representation of column chromatography setup.



**Scanning Electron Microscopy (SEM)**

The surface morphologies of the adsorbents were observed by SEM in Figures 5, 6, 7, and 8 for ACBC and ASBC charcoals, respectively. It is basically a result of the presence of quite a lot of particles in coals. Figures 5 and 6 are for ACBC before and after adsorption. The results obtained from SEM show many pores were created due to the breakage in the surface of the adsorbents before adsorption, while after adsorption it shows little porosity for both adsorbents. This supports the adherence of the metal ion molecules. A similar observation was made in Figures 7 and 8 for ASBC charcoals before and after

adsorption. These changes in morphologies were in good agreement with the literature for various materials (Dawlet *et al.*, 2013; Slimani *et al.*, 2014).

**Column adsorption**

The column adsorption behavior of Pb, Cu, Zn, and Fe metal ions on ACBC and ASBC was studied by varying the temperature, concentration, and contact time. The column adsorption data and parameters for ACBC and ASBC obtained were shown in Tables 3, 4, 5, 6, 7, and 8 of 20ppm, 30ppm, and 40ppm, respectively.

**Table 3: Fixed bed adsorption column data and parameters obtained for metals removal using ACBC.**

Metal Ion Adsorbent Interaction	H (Cm)	Co (Ppm)	Q (ml/min)	T (Sec)	Veff (ml)	% removal
ACBC-Pb	5	20	6.25	480	50	46.2
ACBC-Cu	5	20	2.5	1200	50	37.3
ACBC-Zn	5	20	2.00	1500	50	35.6
ACBC- Fe	5	20	2.00	1500	50	16.60

**Table 4: Fixed bed adsorption column data and parameters obtained for metals removal using ACBC.**

Metal Ion Adsorbent Interaction	H (Cm)	Co (Ppm)	Q (ml/min)	T (Sec)	Veff (ml)	% removal
ACBC-Pb	5	30	7.14	420	50	61.58
ACBC-Cu	5	30	2.78	1080	50	55.9
ACBC-Zn	5	30	2.50	1200	50	56.45
ACBC- Fe	5	30	1.85	1350	50	45.03

**Table 5: Fixed bed adsorption column data and parameters obtained for metals removal using ACBC**

Metal Ion Adsorbent Interaction	H (Cm)	Co (Ppm)	Q (ml/min)	T (Sec)	Veff (ml)	% removal
ACBC-Pb	5	40	6.25	480	50	71.13
ACBC-Cu	5	40	5.00	600	50	64.53
ACBC-Zn	5	40	2.5	1200	50	67.03
ACBC- Fe	5	40	1.85	1620	50	58.53

**Table 6: Fixed bed adsorption column data and parameters obtained for metals removal using ASBC.**

Metal Ion Adsorbent Interaction	H (Cm)	Co (Ppm)	Q (ml/min)	T (Sec)	Veff (ml)	% removal
ASBC-Pb	5	20	2.50	1200	50	25.13
ASBC-Cu	5	20	3.33	900	50	39.1
ASBC-Zn	5	20	2.50	1200	50	49.4
ASBC- Fe	5	20	3.33	900	50	16.80

**Table 7: Fixed bed adsorption column data and parameters obtained for metals removal using ASBC**

Metal Ion Adsorbent Interaction	H (Cm)	Co (Ppm)	Q (ml/min)	T (Sec)	Veff (ml)	% removal
ASBC-Pb	5	30	2.17	1380	50	35.65
ASBC-Cu	5	30	3.33	900	50	56.55
ASBC-Zn	5	30	2.50	1200	50	62.65
ASBC- Fe	5	30	2.50	1200	50	42.65

**Table 8: Fixed bed adsorption column data and parameters obtained for metals removal using ASBC**

Metal Ion Adsorbent Interaction	H (Cm)	Co (Ppm)	Q (ml/min)	T (Sec)	Veff (ml)	% removal
ASBC-Pb	5	40	2.00	1500	50	57.7
ASBC-Cu	5	40	3.33	1500	50	64.90
ASBC-Zn	5	40	3.33	1500	50	69.28
ASBC- Fe	5	40	3.33	1500	50	59.50

**Column adsorption**

The data obtained from Table 5 for adsorption of the metal ions using ACBC indicated that the column

exhaustion time decreases with an increase in concentration; hence the better percentage removal for Pb 71.13% was recorded at 480 secs with a flow rate of 6.25ml/min while Cu 64.53%, Zn 67.03%, and Fe 58.53%

at 10mins, 20mins and 27mins with 5.0ml/min, 2.5ml/min, and 1.85 ml/min flow rate respectively.

**Effect of concentration on the adsorbents**

The influence of initial metal ion concentration was piloted on Pb, Cu, Zn, and Fe using ACBC and ASBC adsorbents. The results given in Table 3, 4 and 5 and Table 6, 7 and 8 show percentages adsorbed at predetermined times corresponding to different initial metal concentrations ranging from 20, 30, and 40 ppm. The initial metal concentration discloses if the adsorption of metal ions on the adsorbent surface happens by growing a monolayer or multilayer. Monolayer adsorption is illustrated by Langmuir isotherm, while multilayer adsorption is expressed by Freundlich isotherm. It can be observed from Table 3, 4 and 5 that the amount of Pb, Cu, Zn, and Fe ions adsorbed increased as the initial metal ion concentration increased for both adsorbents. As the concentration of Pb increased from 20, 30 to 40ppm, there was a corresponding rapid increase in adsorption from 46.2%, 61.58% to 7.13 % for ACBC and an increase from 25.12%, and 35.65% to 57.70% for ASBC. For Cu, there was increase in adsorption from 37.3%, 55.9% to 64.53% for ACBC and an increase from 39.1% and 56.55% to 64.90% for ASBC. A similar increase was revealed for Zn was 35.6%, 56.45% to 67.03%, and 16.60%, 45.03% to 58.53% for ACBC. While 49.4%, 62.5%, and 69.28% Zn and 16.80%, 42.65% and 59.50% for ASBC.

Metal ions adsorbed at equilibrium increase with an increase in concentration, which implies that the initial

concentration of the metal ion influences the adsorption process.

Generally, the initial concentration provides a significant influence, which is key to suppressing all mass transfer resistance between aqueous and solid surfaces, thus a higher initial metal ion concentration, which enhances the sorption process (Pang *et al.*, 2011). The rapid adsorption observed in the early stages is possibly a result of the presence of active sites on the surface of the adsorbents (Fu and Wang 2012). However, the reduction in the percentage removal can be justified by the fact that the adsorbents have an inadequate number of exchangeable sites, which become exhausted above some limits, thereby leaving some adsorbents un-adsorbed (Gueye *et al.*, 2014).

To have an insight into the adsorption behavior of Pb, Cu, Zn, and Fe metal ions against ACBC and ASBC samples and to achieve the best possible fitting of the theoretical model, the experimental data from the column adsorption experiment were analysed using two parameter isotherm equations (Langmuir and Freundlich isotherms), in which linear regression analysis was used to evaluate whether the data fits any of the theoretical models.

**Adsorption isotherms**

The results of adsorption isotherms studies for ACBC and ASBC are presented in Table 9 below, showing the value of all the adsorption isotherms constants corresponding to the adsorption of Pb, Cu, Zn, and Fe metal ions.

**Table 9: Adsorption Isotherms**

Adsorbent Metal ion Interactions	Langmuir isotherm			Freundlich isotherm		
	q <sub>e</sub> (mg/g)	K <sub>L</sub> (l/mg)	R <sup>2</sup>	K <sub>F</sub> (mg/g)	n <sub>f</sub> (g/l)	R <sup>2</sup>
ACBC-Pb	0.0801	0.0173	0.9571	10.256	0.3786	0.999
ASBC-Pb	0.0228	0.0075	0.9919	4.3651	0.1675	0.982
ACBC-Cu	0.1984	0.0408	0.971	6.666	0.5599	1
ASBC-Cu	0.0570	0.0012	0.0899	6.1334	0.3403	0.999
ACBC-Zn	0.1375	0.0015	0.953	1.9588	0.4938	0.999
ASBC-Zn	0.0939	0.0073	0.969	2.5061	0.4178	1
ACBC-Fe	0.0469	0.0092	0.999	6.2517	0.7627	0.942
ASBC-Fe	0.0119	1.1060	0.999	6.3095	0.1712	0.970

**Langmuir Adsorption Isotherm**

The Langmuir isotherm usually ascertains the adsorption process happens by monolayer creation. Langmuir's model deduces identical energies of adsorption onto the surface and denial of transmigration of the adsorbate in the plane of the surface. The Langmuir isotherm is given by Dawlet *et al.*, 2013 as:

$$q_e = \frac{Q^0 b C_e}{1 + b C_e}$$

Where Q<sup>0</sup> and b are Langmuir constants related to adsorption capacity and energy of adsorption, respectively. This equation is usually linearized by inversion to obtain the following form:

$$\frac{1}{q_e} = \frac{1}{Q^0} + \frac{1}{b Q^0 C_e}$$

The equation is equally used to analyze equilibrium data by plotting C<sub>e</sub>/q<sub>e</sub> versus C<sub>e</sub> which yields a linear plot confirmed to the Langmuir isotherm.

## Langmuir Adsorption Isotherm

The Langmuir isotherm is applied to reveal the adsorption process that occurred through monolayer formation. Langmuir isotherm model was verified on the adsorption of Pb, Cu, Zn, and Fe with ACBC and ASBC, and the results were presented in Table 9, which shows the adsorption of (Pb, Cu, Zn, and Fe) having lower regression coefficient value ( $R^2$ ) comparison with  $R^2$  value for Freundlich isotherm. The  $R^2$  values for the adsorption process from Langmuir's model plotted decreases in order ACBC-Fe (0.999), ASBC-Fe (0.999), ASBC-Pb (0.9919), ACBC-Cu (0.971), ASBC-Zn (0.969), ACBC-Pb (0.957), ACBC-Zn (0.953) and ASBC-Cu (0.0899). Elevated values of the regression coefficient,  $R^2$ , confirm that the adsorption followed the Langmuir model. The maximum adsorption capacity was found to increase in order of ACBC-Cu 0.198, ACBC-Zn 0.137, ASBC-Zn 0.0939, ACBC-Pb 0.0801, ASBC-Cu 0.0570, ACBC-Fe 0.0469, ASBC-Pb 0.0228 and ASBC-Fe 0.0119. The dimensionless separation factor  $K_L$  is the measure of favorability of adsorption. The  $K_L$  values for the adsorption of Pb, Cu, Zn, and Fe were found to be 0.0173, 0.0075, 0.0408, 0.0012, 0.0015, 0.0073, and 0.0092 for ACBC-Pb, ASBC-Pb, ACBC-Cu, ASBC-Cu, ACBC-Zn, ASBC-Zn, and ACBC-Fe respectively which indicate that the adsorptions were favorable. On the other hand, the  $K_L$  values for the adsorption of ASBC-Fe were found to be 1.106, which indicates that the adsorption was unfavorable.

## Freundlich Isotherm.

The Freundlich isotherm model has been verified in this research on the adsorption of Pb, Cu, Zn, and Fe on ACBC and ASBC, and the result is presented in Table 9. The Freundlich isotherm supposes that metal ions removal happens on a dissimilar surface by multilayer adsorption and the quantity of adsorbate adsorbed has a reciprocal relationship with the solutes' concentration. It indicates that the adsorption of Pb, Cu, and Zn on ACBC and ASBC follows the Freundlich isotherm for having high values of  $R^2$ . The  $R^2$  values for the adsorption were ACBC-Pb (0.999), ACBC- Cu (1.0), ASBC-Cu (0.999), ACBC-Zn (0.999), and ASBC-Zn (1.0) respectively. The  $K_F$  value for adsorption decreases in the order of ACBC-Pb (10.256), ACBC-Cu (6.660), ASBC-Cu (6.133), ASBC-Zn (2.506), and ACBC-Zn (1.958). However, a higher  $K_F$  value indicates an easy uptake of metal ions from the solution (Ying *et al.*, 2014). The  $n_f$  is an experimental constant related to the degree of the adsorption force. The  $n_f$  values were found to increase in the order of ACBC-Fe 0.762, ACBC- Cu 0.559, ACBC-Zn 0.493, ASBC-Zn 0.417, ACBC-Pb 0.370 and ASBC-Zn with 0.3403, ASBC-Fe 0.171 and ASBC-Pb 0.167. The adsorption process is considered favourable when the

value of  $n_f$  satisfies the condition  $1/ <n_f < 10/$ ; otherwise, it is unfavourable.

## CONCLUSION

This research work has revealed the efficacy of animal bone charcoals (Cow and Sheep) as adsorbents for the removal of toxic metals from aqueous solution using hydrochloric acid as an activating agent. The percentage adsorption for metals increases with an increase in metal concentrations.

The equilibrium data for ASBC-Pb, ACBC-Fe, and ASBC-Fe fit well to the Langmuir isotherm model as demonstrated by high regression coefficient values ( $R^2$ ) 0.999 for each one respectively. While that of ACBC-Pb, ACBC-Cu, ASBC-Cu, ACBC-Zn, ACBC-Zn, and ASBC-Zn fit well to the Freundlich isotherm model with high regression coefficient ( $R^2$ ) value of 0.999, 1.0, 0.999, 0.999 and 1.0 respectively. The adsorption occurs through multilayer formation on the adsorbent surfaces. Also, the values of the Langmuir separation factor  $K_L$  propose that the adsorption procedures are favorable except that of ASBC-Fe which is unfavorable. The Freundlich isotherm constant  $n_f$  for the adsorption of ACBC-Pb, ACBC-Cu, ASBC-Cu, ACBC-Zn, and ASBC-Zn showed adsorption on heterogeneous surfaces.

The FT-IR spectra revealed that the presence of functional groups such as C=O, C-O, OH, and PO<sub>3</sub><sup>-</sup> indicated some modifications in the surface properties of the adsorbents after adsorption as compared to that before adsorption. This expedites the adsorption of adsorbents and metal ions. The SEM images of the adsorbents before adsorption indicated rough surfaces and heterogeneous pore distribution through which the adsorption takes place.

As such, it could be concluded that the animal bones (Cow and Sheep), which are waste materials and very abundant, can be employed to mop toxic metals from aqueous solutions and can serve as a good and efficient adsorbent for water purification and environmental waste treatments in industries. Further studies could be done on the samples' characterization of moisture content, ash content, and pH at zero charge point (pH<sub>zcp</sub>).

## REFERENCES

- Ahmad Y., Yaakub Z., Akhtar P., Sopian K (2015). Production of Biogas and Performance Evaluation of Existing Treatment processes in Palm Oil Mill Effluent (POME). *Renewable and Sustainable Energy* (5); 1260-1278. [\[Crossref\]](#)
- Alicia, A., Palaezcid A., Benemerita M. M., Dr Virginia H. M. (2012). Lignocellulosic Precursors used in the synthesis of Activated Carbon Characterization Techniques and Applications in the Wastewater Treatment. *Journal of Engineering and Applied Sciences*, 2(2): PP. 440-444. ISBN: 978-953-51-0197-0.

- Braukmann, B.M., (1990). Industrial Aolution Amenable to Biosorption. In Biosorption (Edited by Volusky B),CRC Press, Boca Raton, FL.*Journal of Chemical Technology and Biotechnology*.54:3937.
- Dawlet, A., Dilnur, T., Hong, Yu M., Malikezha T., (2013). Removal of Mercury from Aqueous Solution using Sheep Bone Charcoal. *International Symposium on Environmental Science and Technology Procedie Environment Sciences* (18); 800-808. [\[Crossref\]](#)
- Fu, F.and Wang, Q. (2011). Removal of Heavy Metal ions from Waste Waters: *A Review Journal of Environmental Management*, (92); 407-418. [\[Crossref\]](#)
- Gueye, M, Richaradson, Y, Kafack, F.T. and Blin, J. (2014). High Efficiency Activated Carbons from African Biomass Residues for the Removal of Chromium (VI) from Wastewater. *Journal of Environment Chemistry*, (2); 273-281. [\[Crossref\]](#)
- Gumus, E., Laghdach, E. Manuel Cuerda Correa, M. Stitou, F. Jbari (2012). Preparation of Bone Chars by Calcinations in Traditional Furnance. *Journal of Material Environmental Science*.(5);, 476-483.
- Handayani, L. Nurhayati, Syahputr, F. Thaib, A. Astuti, Y. Darmawan, A. Mardhiah, A. (2024). Characterization Charcoal and Activated Carbon from Starry Triggerfish (*Abalistes stellaris*) Bone Activated using Zinc Chloride to Reduce Cr<sup>6+</sup> *Agrointek* **18** (4) 1019-1026
- Kenith, K.H., Mekay, G. (2008) Study of Arsenic (v) Adsorption on Bone Char from Aqueous Solution; *Hazard Mater*, (1); 160, 845-854. [\[Crossref\]](#)
- Idris, M.A., Jamal, M.S. and Muyibi, S.A. (2010). Tertiary Treatment of Biologically Treated Palm Oil Mill Effluent (POME) using UF Membrane System: Effect of MWCO and Transmembrane Pressure. *International Journal of Chemistry Environmental and Engineering*(1); 108-112.
- Isaial, O. A. and Frank, E O. (2024). Production of Activated Carbon from Cow Bone for the Purification of Water. *International Research Journal of Modernization in Engineering Technology and Science* 4049-4054 e-ISSN: 2582-5208
- Jorie, N., Jacquillet, G., &Unwin, R (2010). Heavy Metals Poisoning: The Effects of Cadmium on Kidney. *Bio Metals*, (1); 783- 792. [\[Crossref\]](#)
- Keith, K.H., and Mekay, G. (2008) Study of Arsenic (v) Adsorption on Bone Char from Aqueous Solution; *Hazard Mater*, (1); 160, 845-854. [\[Crossref\]](#)
- Lourie, E, Patil, V. and Gjengendal E (2010). Efficient Purification of Heavy Metals Contaminated Water by Micro Algae Activated Pirie Bark. *Water, Air, Soil pollut*, (1); 210, 493-500. [\[Crossref\]](#)
- Moshood, T O., Balogun, A. A. Odeh, L. U. Udoh, E. A. Mohammed, A. Omolusi, A. R. Ankomah, N. O. Akyea-Mensah, S. B., Onele, E. J., Akoh, M. D. (2024). Production and Characterization of Activated Carbon from Coconut Shell for Adsorption of Lead (II) Ion from Waste Water. *Advanced Journal of Chemistry, Section B, Natural Products and Medical Chemistry*, 2024, 6(3), 269-283
- Nwankwo, I.H.1., Nwaiwu, N. E.and Nwabanne, J.T. (2018). Production and Characterization of Activated Carbon from Animal Bone. *American Journal of Engineering Research (AJER)*. **7**(7)335-341
- Pang, F.M, Kumar, P., Teng, T.T, Mohd Omar, A.K. and Wasewar, K.L. (2011). Removal of Lead, Zinc and iron by Coagulation- Flocculation. *Journal of the Taiwan Institute of Chemical Engineers*, (42); 809-815. [\[Crossref\]](#)
- Saad, S.M. Hassan, Awaad, H.A., Aboterika, and Nasser S. A. (2008). Removal of Mercury (II) from Waste Water using Camel Cone Charcoal. *Journal of Hazard Materials*, **54** (1) 992- 997. [\[Crossref\]](#)
- Slimani A.N.,Laghdach,A.E.I., Manuel, C. C.E., Stitou,M. and Jbari, F. (2013). Preparation of Bone Chars by Calcinations in Traditional Furnance. *Journal of Material Environmental Science*.(5); 476-483.
- WHO, World Health Organisation. 2001.
- Yildiz, E. (2004). Phosphate Removal from Water by Fly as using Crossflow-Micro-Filtration *Purif. Technol.*, 35, 241-252. [\[Crossref\]](#)
- Zulaikha, S. N. Kadoura, A. M. Alkbir, M.F.M., Mohammad, Z., Kosnan, S. E., Januddi, F. (2023). Surface Porosity Enhancement of Activated Carbon by Synthesizing Kenaf Fiber. *International Journal of Intelligent Systems and Applications in Engineering*. **12**(9s), 136–141.